Chapter 5

Thermal Barrier Ceramic Coatings — A Review

Sumana Ghosh

Additional information is available at the end of the chapter

http://dx.doi.org/10.5772/61346

Abstract

Thermal barrier coatings (TBCs) provide effective thermal barrier to the components of gas turbine engines by allowing higher operating temperatures and reduced cooling requirements. Plasma spraying, electron-beam physical vapor deposition, and solution precursor plasma spray techniques are generally used to apply the TBCs on the metallic substrates. The present article addresses the TBCs formed by different processing techniques, as well as the possibility of new ceramic, glass-ceramic, and composite materials as TBCs. Promising bond coat materials for a TBC system have been also stated.

Keywords: Processing techniques, new TBC materials, engine applications

1. Introduction

Thermal barrier coatings (TBCs) enable the engines to operate at higher temperatures without raising the base metal temperatures using cooling systems inside the hot section components and thus, enhance the operating efficiency of the engines [1]. Therefore, continued development of TBCs is essential to increase the inlet gas temperature further for improving the performance of gas turbines. Hence, TBCs with low thermal conductivity, phase stability, and high resistance to sintering have ever increasing demands [2]. Generally, TBCs consist of a ceramic (e.g., yttria partially stabilized zirconia) top coat and a NiCoCrAlY/PtAl-based metallic bond coat. A bond coat is deposited between the metallic substrate and the top coat to protect the metal substrate from oxidation and high temperature corrosion and assist the coupling of the ceramic top coat and the metallic substrate [3]. Two methods are generally used to deposit the ceramic top coat. These are the electron beam physical vapor deposition (EB-PVD) and the atmospheric plasma sprayed (APS) methods. TBCs with EB-PVD top coats generally provide longer thermal cycle lifetimes because of its more strain-tolerant columnar structure than those observed with APS TBCs. However, APS TBCs are widely applied due to lower thermal

conductivity and lower processing costs [3]. Recently, various processing techniques have been developed to deposit the ceramic coatings.

The objective of this article is to present an overview of the TBC requirement, application of TBCs, degradation mechanisms for TBCs, different processing techniques used for preparation of TBCs, and their thermal properties. Recent developments in TBC material have been also described. The prospect of innovative materials as bond coat in a TBC system has been elucidated.

2. Main requirements for TBCs

TBCs must have low weight and low thermal conductivity and they should withstand large stress variations due to heating and cooling, as well as thermal shock. They must be chemically compatible with the underlying metal and the thermally grown oxide (TGO) and should operate in an oxidizing environment. TBCs must provide thermal insulation to the underlying superalloy engine parts. They must have strain compliance in order to minimize the thermal expansion mismatch stresses with the superalloy parts. Additionally, they must reflect much of the radiant heat from the hot gas and thereby, preventing it from reaching the superalloy substrate. Further, TBCs must provide thermal protection to the substrate for prolonged service times and thermal cycles without failure [4].

3. Applications of TBCs

TBCs provide thermal insulation to superalloy engine parts such as the combustor, rotating blades, stationary guide vanes, blade outer air-seals, shrouds in the high-pressure section behind the combustor, and afterburners in the tail section of jet engines. Significant gas-temperature increase can be achieved by using TBCs in association with innovative air-cooling approaches than that obtained by earlier materials including single-crystal Ni-based superalloys [4].

4. Degradation mechanisms

During service, several kinetic processes occur in parallel. Interdiffusion occurs between the bond coat and the superalloy. Consequently, Al diffuses from the bond coat to form the TGO. Microstructural, chemical, and phase changes occur in all the materials including the ceramic top coat. The rates of these thermally activated processes are expected to increase exponentially with temperature. These processes generally lead to degradation and failure of the coating [5]. During service, failure of the TBC system occurs depending upon the following three factors:

http://dx.doi.org/10.5772/61346

4.1. Bond coat degradation

Bond coat plays an important role in promoting the durability of the TBC system. But the role of the bond coat is very complex and poorly understood. In most practical cases, oxidation of the bond coat becomes the predominant coating failure mechanism. During high temperature exposure, NiCrAlY bond coat is oxidized resulting in a TGO layer on the bond coat. After reaching a critical thickness, the TGO becomes prone to spallation, which in turn results to the failure of the TBC system. It is very difficult to establish the exact mechanisms of bond coat-induced TBC failure for various coating types. However, all researchers agree on the significance of spallation or cracking of the TGO for the failure of air plasma-sprayed TBC system. Detailed research is being conducted to find out a solution to the problem regarding bond coat degradation in the TBC system [5]. Nanostructured NiCrAlY bond coat may improve the life expectancy of thermal barrier coatings. Daroonparvar et al. [6] investigated the microstructural evolution of TGO layer on the conventional and nanostructured atmospheric plasma sprayed (APS) NiCrAlY coatings in TBC systems during oxidation. It was observed that the growth of $Ni(Cr,Al)_2O_4$ (as spinel) and NiO on the surface of the Al_2O_3 layer (as pure TGO) in nano TBC systems was much lower compared to that of normal TBC systems during thermal exposure at 1,150°C. These two oxides play a detrimental role in causing crack nucleation and growth, reducing the life of the TBC in air. This microstructure optimization of the TGO layer is primarily associated with the formation of a continuous, dense, uniform Al_2O_3 layer over the nanostructured NiCrAlY coating [6]. The interfacial failure mechanism of the TBC system was numerically investigated by Xu et al. [7], considering the role of mixed oxides (MO), which was induced by the discontinuous α-Al_2O_3 at the top coat-bond coat interface. High growth rate of MO will stimulate the initiation and propagation of interface cracks resulting in debonding of the top coat. The high coverage ratio of MO at the interface will accelerate the propagation of an interface crack. Therefore, the durability and performance of TBCs can be improved by suppressing the formation of MO [7]. The prediction for spallation of thermal barrier coatings has proven to be an intricate problem [8]. The spallation usually occurs through buckling that is driven by strain energy release within the ceramic top coat. If the delamination interface is at the bond-coat/TGO interface, then spallation occurs within the underlying TGO layer. Prior to spallation, substantial sub-critical damage must develop at one or both of the TGO interfaces. Evans [8] stated that the strain energy within the TGO produced during cooling contributes significantly to this damage development and not that within the top coat. Critical strain energy within the TGO layer is assumed to be a possible pragmatic method of predicting the spallation. Several factors such as phase changes in the bond coat, mechanical constraint imposed by the top coat on the mechanical stability of the bond coat interface, TGO growth on a non-planar interface on stress development, and localized Al depletion in nucleating fast-growing non-protective TGO influence the TBC failure [8].

4.2. Generation of high residual stress

Residual stress has a vital effect on the performance of a TBC system. The role of residual stress is very complex and varies with the difference in system configurations. Thermal expansion mismatch between the three layers generates residual stress resulting in degradation of a TBC

system. Although extensive research has been initiated to study the effect of residual stress on TBC life, there is still ample scope to carry out this study on novel TBC systems involving novel compositions [9]. High residual stresses are induced in the TBC due to thermal expansion mismatch and bond coat (BC) oxidation leading to failure by spalling and delamination. An analysis of the stress distributions in TBC systems, which is a prerequisite for the understanding of failure mechanisms, was performed by Sfar et al. [10] using the finite element method (FEM). Cracks in the interface region were considered in the FE models in order to determine the loading conditions for their propagation and thus, the failure criteria of the TBCs as cracking usually occurs at or near the interfaces between BC/TGO and TBC/TGO depending on the processing mode of the TBC. The modified crack closure integral (MCCI) method combined with an FE analysis led to highly accurate energy release rate values. Moreover, this method enables the determination of mode-dependent energy release rates. TBC failure models could be developed and verified using this tool and appropriate crack propagation criteria [10]. Yang et al. [11] investigated the residual stress evolution in air plasma-sprayed yttria-stabilized zirconia (YSZ) TBCs after thermal treatments at 1,150°C. The residual stress in the YSZ layer was measured using Raman spectroscopy and the curvature method. Generally, as-deposited YSZ layer was under compressive stress and subsequently after thermal treatment for 30 h it was under tensile stress partly due to the monoclinic to tetragonal phase transformation in the YSZ layer. Sintering of the YSZ layer occurred with prolonged thermal treatment resulting in the gradual transformation of the residual stress, from tensile to compressive stress. Further, β-NiAl to γ/γ'-Ni_3Al phase transformation in the bond coat also plays an important role on the stress development in the top coat [11].

4.3. Top coat degradation

Top coat degradation is another parameter that governs TBC failure. The ceramic top coat has a tendency to crack due to stress generated from thermal expansion mismatch between the three layers of the TBC system. When the top coat cracks, oxygen easily diffuses to the bond coat leading to the catastrophic failure of the TBC system. Significant research is being carried out to improve the microstructure, mechanical properties, and stability of the ceramic top coat [12]. TBCs are subject to many kinds of degradation, e.g., erosion, foreign object damage (FOD), oxidation, etc., which deteriorate the integrity and mechanical properties of the whole system. Moreover, a new type of damage has been highlighted, i.e., corrosion by molten Calcium-Magnesium-Alumino Silicates, known as CMAS with the aim to increase the turbine inlet temperature. Basu et al. studied interactions between YSZ materials synthesized via the sol-gel process and synthetic CMAS powder via a step-by-step methodology. However, CMAS can cause faster sintering of the ceramic and thereby, leading to loss of strain tolerance in the protective coating. Further, a dissolution/re-precipitation mechanism between YSZ and CMAS resulted in the transformation of the initial tetragonal YSZ into globular particles of monoclinic zirconia. In addition, CMAS infiltrated both EB-PVD and sol-gel YSZ coatings at 1,250°C for 1 h [12]. Thompson and Clyne [13] deposited a vacuum plasma spray (VPS) MCrAlY bond coat and atmospheric plasma spray (APS) zirconia top coat onto a nickel superalloy substrate. They measured the stiffness of detached top coats by cantilever bending and also by nanoindentation technique. Measurements were made on as-sprayed specimens and after various

http://dx.doi.org/10.5772/61346

heat treatments. Significant changes were detected in the Young's modulus of the heat treated top coat. The rate of sintering was found to be a function of temperature and weather. The coating was detached with the substrate during heat treatment. During high temperature exposure the effects of stiffening of the top coat on the stress development within the TBC system was included by using a well-known, modified numerical model. Sintering of the top coat enhanced debonding at the top coat-bond coat interface resulting in top coat spallation under service conditions [13]. It has been found by Abubakar et al. [14] that the use of low grade fuels in land-based turbines in Saudi Arabia results in hot corrosion due to the diffusion of a molten salt (V_2O_5) into the top coat of the TBCs. Consequently, volumetric expansion of the coating occurs due to the tetragonal-to-monoclinic transformation of zirconia in the planar reaction zone near the surface of the coating. They used a phase field model for estimating the kinetics of microstructure evolution during the corrosion process at 900 °C and close agreement between numerical and experimental results was achieved. The transformation-induced stresses were predicted by coupling the phase transformation with elasticity. The result showed that the coating spallation occurred due to very high compressive stress development within the coating cross section [14].

5. Processing techniques for TBCs

5.1. EB-PVD process

In the EB-PVD process, the source material is heated with an electron beam, vapors are produced, and the evaporated atoms condense on the substrate. Crystal nuclei form on favored sites and grow laterally and in thickness to form individual columns that provide in-plane compliance [15]. A TGO layer often forms on the bond coat in these TBC systems and increases the residual stress. Further, brittleness of the top coat increases with the sintering of the coating. Consequently, the adhesion of the bond coat to the top coat becomes weak at high temperatures. Therefore, the TGO layer is very detrimental for TBC performance [16]. Movchan and Yakovchuk [17] described the design of a new generation of electron beam units for the deposition of the TBCs and cost-effectiveness of the one-step deposition process. They produced variants of graded TBC, which consist of bond coats of NiAl or MCrAlY+NiAl and YSZ-based outer ceramic layer in a one-step cycle by evaporation of a composite ingot. The composition and structure of the bond coats, outer ceramic layer, and the transition barrier zones of the substrate/bond coat and bond coat/outer ceramic layers was controlled in a broad range. They have shown distributions of chemical elements in the coating/substrate system and microstructure after deposition and after heat treatment. Various types of graded TBCs were subjected to thermal cycling tests at 1,150°C and their thermal cyclic resistance was monitored [17]. Current numerical approaches in modeling the intrinsic failure of TBC relies largely on the fact that spallation occurs when the accumulating strain energy stored in the coating exceeds a fixed critical value resembling interfacial adhesion. If this is to be entirely correct, one would expect that this critical value of interfacial adhesion varies with different materials, but stays independent of their thermal exposure history. Wu et al. [18] characterized the adhesion of oxide-bond coat interface among five systematically prepared material systems

using a unique cross-sectional indentation technique. The results re-confirmed that interfacial adhesion is a material-specific property and the adhesion is dynamic, particularly with time and temperature. Certain parameters such as the oxide growth rate, rumpling of the oxide-bond coat interface, and phase transformation of bond coat were studied as a function of thermal exposure to understand the dynamics. They clearly indicated that the oxide-bond coat interfacial adhesion depends strongly on the phase distribution of the bond coats and TGO growth rate while having little effect from TGO rumpling and residual stress [18].

5.2. APS process

In the APS process, ceramic powders are introduced into a high temperature plasma plume, melted inside the plume, and accelerated towards the substrate wherein molten droplets spread and form splats that are rapidly quenched. In one pass, several successive splats are deposited on the substrate and the coating thickness is increased by means of several passes [19]. A typical fractured cross-section of the plasma sprayed ceramic coating show layers of splats along with interlamellar pores, cracks, and globular pores [15]. Coating compliance is increased by the presence of the cracks and thereby, extending their lifetimes [19]. The resulting coating microstructure is strongly dependent on processing conditions such as spray parameters (e.g., torch current, plasma gas flow rate, carrier gas flow rate, torch traverse velocity, and stand off distance) and feedstock materials (e.g., size, temperature, and velocity). Splat morphologies are changed with the angle of impact of impinging particle [15]. Higher substrate temperatures lead to lower porosity and improved inter-splat contact resulting in enhanced coating properties [20]. During service operations at high temperatures, a TGO layer, mainly an Al_2O_3 layer, is developed between the bond coat and the top coat due to the oxidation of the bond coat. This is the most important factor that determines the lifetime of the TBC system. The thickness of this layer increases with increasing operation time. High stresses are present at the bond coat and TGO interface because of oxide layer growth, thermal expansion misfit, and applied loads. As a result, crack initiates and propagates resulting in spallation of the ceramic layer, and finally, system degradation [3]. During thermal exposure at ≥1,000°C, Ni(Cr, $Al)_2O_4$ (spinels) and NiO clusters are also formed at the interface of the Al_2O_3 layer and the ceramic coating in the TBC system with MCrAlY (M=Ni, Co) bond coat. Cracks were nucleated on these oxide clusters and grew into the ceramic coating leading to premature TBC separation. A heat treatment in a low pressure oxygen environment was found to promote the formation of a uniform, thin protective layer of Al_2O_3 at the ceramic-bond coat interface and can reduce these detrimental oxides [21].

Thermo-mechanical properties of TBCs have been studied to improve TBC performance. The Young's modulus of the ceramic top coat is an important factor that affects the thermal stress distribution in TBCs and thus, thermal fatigue behavior. Apparent Young's modulus (E_{ap}) indicates the macro-elastic properties of the coatings. E_{ap} of the top coat is usually much lower than the value for dense YSZ due to the porous microstructure. The extremely low E_{ap} values are also attributed to the weak bonding between the particles because of the extremely high cooling rate. Tang and Schoenung [22] conducted bending tests of the TBC specimens exposed to thermal cycling to determine their E_{ap}. The E_{ap} decreased with increasing thermal cycles, up

http://dx.doi.org/10.5772/61346

to certain thermal cycles, and then remained unchanged for increased thermal cycles. The breaking of the bonds at the splat boundaries or the formation of new cracks caused by thermal strain is the reason for the decrease in E_{ap} with increasing thermal cycles. Effect of heat treatment on the elastic properties of the separated porous plasma sprayed zirconia TBCs was investigated by D. Basu et al. [23]. The depth-sensitive indentation technique was employed to determine the elastic moduli of the coatings. The characteristic moduli were dependent on the indentation load. The increase of moduli with decreased indentation load was attributed to the presence of small pores and micro-cracks at the subsurface. Heat treatment of the coatings at 1,100°C increased the elastic moduli appreciably due to the formation of sintering necks and the elimination of the micro-pores within the lamellae.

Functionally graded Al_2O_3–ZrO_2 TBC was prepared by plasma spraying technique and reported elsewhere [24]. Functionally-graded TBC was found to reduce the oxidation rate of the TBC system. Thus, large residual stress associated with the formation of TGO was minimized. The Al_2O_3 interlayer should be very thin to increase the adhesion of the layers. However, low fracture toughness of Al_2O_3 might lead to TBC failure. In addition, phase transformation of γ-Al_2O_3 to α-Al_2O_3 could induce additional residual stress, which should be minimized to get reliable TBC systems. Thick thermal barrier coatings (thickness >1 mm) have been developed for increased thermal protection by using the APS method [25]. However, low thermal shock resistance is the problem with the thick coating. Certain degrees of porosity and micro-cracks, preferably segmentation cracks, in TBCs favor to achieve high thermal shock resistance. Chen et al. [26] prepared a new functionally-graded thermal barrier coating based on $LaMgAl_{11}O_{19}$ (LaMA)/YSZ by using air plasma spraying technique. The coefficient of thermal expansion (CTE) of the functionally-graded coating varied gradually from the YSZ bottom layer to the LaMA top layer, resulting in the decrease in residual stress level than that of the LaMA/YSZ double ceramic layered TBC system. Excellent thermal cycling lifetime (~11,749 cycles at~ 1,372°C) of the functionally graded TBC proved the potential of these TBCs for advanced applications [26].

5.3. Plasma-Enhanced Chemical Vapor Deposition (PECVD) method

Thick, partially yttria-stabilized zirconia coatings have been deposited by plasma-enhanced chemical vapor deposition (PECVD) method. The morphology and phase composition of the coatings was studied after annealing treatments at the temperature range of 1,100 to 1,400°C up to 1,000 h. The as-deposited columnar morphology of the coating was similar to that observed in the coating prepared by the EBPVD technique. The PECVD method is suitable for developing TBCs as it provides thermally stable coating at elevated temperatures [27].

5.4. Electrostatic Spray-Assisted Vapor Deposition method (ESAVD)

TBCs, such as 8 wt. % Y_2O_3–ZrO_2 (YSZ), provide effective thermal barrier to the gas turbine blades and are able to protect them, leading to further increase in the operating temperature. A novel and cost-effective electrostatic spray-assisted vapor deposition (ESAVD) technique was utilized to prepare YSZ coatings, which involves spraying atomized zirconium and yttrium alkoxide precursor droplets within an electric field wherein they are subjected to

decomposition and/or chemical reactions in the vapor phase near the heated substrate. The coatings were characterized by scanning electron microscopy, X-ray diffraction, and Raman spectroscopy. Vyas and Choy [28] produced thick and uniform YSZ films using the ESAVD method. Raman spectroscopy identified carbon to be present in the as-deposited coatings. When heat treatment of the YSZ coating was conducted at 1,000°C for 2 h, carbon was removed and the adhesion of the TBC coating to the bond coat improved [28].

5.5. Solution-Precursor Plasma Spray (SPPS) process

In this process, an aqueous chemical precursor feedstock is injected into the plasma jet where the droplets undergo a series of physical and chemical reactions and then deposited on the substrate as coating. Microstructural observations of this type of TBC show fine splats and vertical cracks in a porous matrix. TBCs deposited by the optimized solution-precursor plasma spray (SPPS) process exhibit superior durability relative to TBCs formed by the APS and EB-PVD processes. Thick and durable TBCs can be deposited by this process. Failure of these TBCs occurs by large scale buckling of the ceramic top coat [29]. The efficiency of TBCs used to protect and insulate metal components in engines increases with the thickness of the TBCs. However, the durability of thick TBCs deposited using conventional deposition methods has not been adequate. Jadhav et al. [30] deposited highly durable, 4 mm-thick ZrO_2–7 wt% Y_2O_3 (7YSZ) TBCs on bond-coated superalloy substrates using the SPPS method. The average thermal cycling life of the SPPS TBCs was 820 cycles, while most of the conventional air plasma-sprayed coatings of the same composition and thickness deposited on similar bond-coated superalloy substrates were observed to be detached partially from the substrates in the as-sprayed condition. Only the APS TBC failed after 40 thermal cycles. Significantly higher in-plane indentation fracture toughness and high degree of strain tolerance due to the presence of the vertical cracks in the SPPS TBCs led to the dramatic improvement in the thermal cycling life of the SPPS TBCs over APS TBCs [30].

5.6. Sol-gel process

Recently, a new, attractive sol-gel route has been successfully developed to synthesize and deposit the TBCs [31–34]. Non-directional deposition and formation of thin or thick coating by dip or spray technique or the combined method of both techniques can be performed by this technique. Sol-gel TBCs show an isotropic microstructure having randomly distributed porosities leading to a good compromise between thermal conductivity and mechanical strength. The degradation of sol-gel TBCs is initiated by the formation of a regular crack network either during the post-deposition thermal treatment required to sinter the deposit or during the first cycles of oxidation. In both cases, this regular surface crack network forms on account of the in-plane stress release due to the sinter-induced shrinkage of the zirconia scale. Subsequently, enlargement and coalescence of the cracks occur under cumulative oxidation cycles promoting the detachment of individual TBC layers and finally, the complete spallation of the TBC. To improve the cyclic oxidation resistance of the TBCs, the sintering efficiency after the TBC deposition needs to be improved or the crack network needs to be stabilized by filling crack grooves by supplementary dip or spray coating passes [33]. In addition, the feasibility

of consolidating sol-gel TBCs by additional fillings of zirconia into the sinter-induced cracks was investigated by adjusting different process parameters such as the choice of either dip-coating or spray-coating and the modification of the slurry viscosity [34]. Basically, the optimization of both the sintering heat treatment and the procedure for filling the initial crack network promotes a significant improvement of the sol-gel TBC durability during cyclic oxidation at 1,100°C. Typically, a sol-gel TBC that is properly sintered and adequately reinforced can be cycled for 1 h at 1,100°C one thousand and five hundred times without spalling, which is nearly equivalent to the performance of EB-PVD TBCs [33, 34].

5.7. Composite sol-gel method

Composite sol-gel method and pressure filtration microwave sintering (PFMS) technologies were utilized to form novel YSZ (ZrO_2–6 wt% Y_2O_3)–(Al_2O_3/YAG) (alumina–yttrium aluminum garnet, $Y_3Al_5O_{12}$) double-layer ceramic coatings. The thin Al_2O_3/YAG layer showed good adhesion with the substrate. Cyclic oxidation tests were carried out at 1,000°C, which indicated that double-layer ceramic coatings can prevent the oxidation of alloy and improve the spallation resistance. The 250 μm coating had better thermal barrier effect than that of the 150 μm coating during thermal stability tests at 1,000°C and 1,100°C at different cooling gas rates. These beneficial effects are mainly attributed to the decrease of the rate of TGO scale development and the reduced thermal stresses by means of nano/micro-composite structure. This double-layer coating can be considered as a promising TBC [35].

5.8. Spark Plasma Sintering (SPS) method

Pt-modified Ni aluminides and MCrAlY coatings (where M=Ni and/or Co) are widely used on turbine blades and vanes for protection against oxidation and corrosion and as bond coat in TBC systems. The SPS method can be used by Monceau et al. [36] to develop rapidly new coating compositions and microstructures. This technique allows the formation of multi-layered coatings on a superalloy substrate. They have shown the possibility of fabricating MCrAlY overlays with local Pt and/or Al enrichment and coatings made of ζ-$PtAl_2$, ε-PtAl, α-$AlNiPt_2$, martensitic β-(Ni,Pt)Al, or Pt-rich γ/γ′ phases. Further, they have demonstrated the prospect of achievement of a complete TBC system with a porous and adherent YSZ layer on a γ/γ′ low mass bond coating. Additionally, they have discussed the difficulties of fabrication such as Y segregation, risks of carburization, local overheating, or difficulty to coat complex shape parts [36]. Recently, Boidot et al. [37] prepared complete TBC systems on single crystal Ni-based superalloy substrate in a one-step SPS process. A proto-TGO layer in situ was formed during the fabrication of the TBC systems. Formation of a dense, continuous, slow-growing alumina layer (TGO) between a ceramic top coat and an underlying bond coat during service influences the lifetime of the TBC systems. During thermal treatment at 1,100°C in air, the amorphous oxide layer transforms to α-Al_2O_3 in the as-deposited samples. Oxidation kinetics during annealing was in good agreement with the protective α-Al_2O_3 layer formation [37]. In the last decade, an increasing interest was given to Pt-rich γ–γ′ alloys and coatings as they have shown good oxidation and corrosion properties. SPS has been proved to be a fast and efficient tool to fabricate coatings on superalloys including entire TBC systems. Selezneff et al. [38] used the SPS technique to fabricate doped Pt-rich γ–γ′ bond coatings on the superalloy

substrate, whereas the doping elements were reactive elements (e.g., Hf, Y or Zr, Si) and metallic additions of Ag. These samples were then coated with Y-PSZ TBC through the EBPVD method. The performance of such TBC system was compared to a conventional TBC system consisting of a β-(Ni,Pt)Al-based bond coat. Thermal cycling tests were performed in air and spallation was observed during this test. It was noted that most of the Pt-rich γ–γ′ samples showed better adherence of the ceramic coating than that of the β-samples. Cross-sectional scanning electron microscopy was used to characterize the thickness and the composition of the oxide scales after cyclic oxidation test. It was proved that the doping elements have significant influence on the oxide scale formation, metal/oxide roughness, Al and Pt content under the oxide scale, and TBC adhesion. It was established that RE-doping can not improve the oxidation kinetics of Pt-rich γ–γ′ bond coat. Moreover, γ–γ′-based systems were superior to β-(Ni,Pt)Al bond coat with respect to ceramic top coat adherence and better oxide scale adherence [38].

5.9. Low-pressure plasma spraying process

The TBC must exhibit high thickness (100–300 μm), vertical cracks should be present in the TBC in order to be a strain tolerant layer, and it must have high porosity to decrease the thermal conductivity. Rousseau et al. [39] prepared a Y-PSZ layer using low-pressure plasma spraying technique by introducing a solution of nitrate salt into a low-pressure plasma discharge. The characteristics and stability of the Y-PSZ layers were analyzed by several techniques. Optical emission spectroscopy indicated that the oxidant chemistry of the plasma caused oxide formation and the nitrate elimination at low temperature (T<300°C). Effects of the several parameters such as power of the plasma discharge, post-treatment and heat treatment on structure, morphology, and stability of the Y-PSZ coatings was studied by X-ray diffraction (XRD), scanning electron microscopy (SEM), water porosimetry, and thermal diffusivity measurement. It was observed that Y-PSZ coating (porosity-50%) had good thermal barrier property at high temperatures [39].

5.10. Thermal plasma process

Superior properties such as high-melting point, high phase stability, low sintering ability, low thermal conductivity, and low oxygen permeability of lanthanum zirconate (LZ) have made it one of the most promising TBC materials for high-temperature applications. However, the production methods used to synthesize lanthanum zirconate are highly time-consuming and the powder is not commercially available. Hence, the thermal plasma process was utilized to synthesize, spheroidize, and spray deposits of lanthanum zirconate material by Ramachandran et al. [40]. They demonstrated the effectiveness of thermal plasma as a major materials processing technique. Suitable characterization techniques were used to study the material modifications after respective plasma processing exposures [40].

5.11. Cathodic Plasma Electrolytic Deposition (CPED) method

Inconel alloys (IN738) have a wide range of applications in industries as high temperature structural materials. Further, different surface treatments and coatings have been developed

for the improvement of the properties of Inconel alloys. Bahadori et al. [41] deposited Al_2O_3 ceramic coating on MCrAlY bond-coated Ni-based superalloy using the CPED method in an ethanol solution of Al $(NO_3)_3.9H_2O$ (18 g/l). Several samples were prepared under different deposition conditions and characterized by XRD, SEM, and energy dispersive X-ray spectrometer (EDS). The XRD analysis confirmed the presence of Al_2O_3 and Ni_3Al phases. The results were in good agreement with the composition of the MCrAlY bond coat based on the thermal expansion data. SEM micrograph showed changes in the microstructure of the specimen by varying the pH of the solution [41].

5.12. Detonation gun spray technique

Kim et al. [42] had taken a new approach and fabricated an excellent functionally-graded thermal barrier coating (FGM TBC) by using the detonation gun spray process in association with a newly-proposed shot-control method. FGM TBCs were sprayed in the form of multi-layered coatings having a compositional gradient across the thickness. FGM TBCs consisted of a finely mixed microstructure of metals and ceramics with no interfaces between the layers. The gradient ranged from 100% NiCrAlY metal on the substrate to a 100% ZrO_2–8 wt% Y_2O_3 ceramic for the topcoat. In the FGM layer of the FGM TBCs, the ceramics and metals maintained their individual properties without any phase transformation during the spraying process. They investigated the thermal shock properties of FGM TBCs and compared the data obtained with those for traditional duplex TBCs [42].

5.13. Plasma laser hybrid spraying technique

Post-treatments of sprayed coatings and simultaneous spraying processes by a plasma laser hybrid technique have been tried by Chwa and Akira [43] to improve the lifetime of TBC coatings. An analytic technique using a low-viscosity resin with a fluorescent dye under a high vacuum has been investigated for the accurate observation of the microstructure of TBCs prepared by a post-laser treatment and a laser hybrid spraying process. Coatings formed by post-laser treatments and laser hybrid spraying processes showed significantly improved thermal shock resistance compared to as-sprayed coatings as a consequence of water quenching tests. The relationship of the microstructure of TBCs modified by laser treatment and thermal shock resistance has been evaluated by the careful observation of samples. They suggested the optimum process conditions for improving the thermal shock resistance of TBCs [43].

5.14. Electrophoretic deposition method

Wang et al. [43] synthesized Gd_2O_3 doped 4-YSZ (G-YSZ) ceramic coatings by electrophoretic deposition method followed by vacuum sintering and isothermally annealing at 1,000°C for different times. XRD was used to investigate their phase composition. SEM was employed to examine their microstructure, while EDS was used to assess the composition of the composite coatings. The results showed that YSZ coating was composed of tetragonal and monoclinic phases after vacuum sintering at 1,000°C for 2 h under vacuum ($<10^{-3}$ Pa). G-YSZ composite coatings were composed of tetragonal and monoclinic phases and a small amount of

$Gd_2Zr_2O_7$ phase after vacuum sintering at 1,000°C for 2 h while the content of the monoclinic phase in G-YSZ composite coatings increased with the increase of Gd_2O_3 concentration. It was found that after isothermal annealing at 1,000°C in air for 100 h, G-YSZ composite coatings were composed of tetragonal ZrO_2 phase, monoclinic ZrO_2 phase, and cubic phase whereas the $Gd_2Zr_2O_7$ phase disappeared [44].

6. Relatively new developments of TBC materials

6.1. Ceramic top coat

Vassen et al. [45] investigated three zirconate materials as potential TBC materials. They deposited 150 μm Ni-Co-Cr-Al-Y bond coat on IN738 substrate before deposition of zirconate (thickness-240 μm) as top coat. They indicated that $SrZrO_3$ can not be used as a top coat in TBC systems as the coating showed a phase transition with a volume expansion at ~730°C that led to the failure of the samples. $BaZrO_3$ showed relatively poor thermal and chemical stability resulting in early failure in thermal cycling tests. On the other hand, Young's modulus of the pyrochlore $La_2Zr_2O_7$ was found to be lower than that of YSZ. Fracture toughness of this material was comparable to the toughness of plasma-sprayed YSZ coatings. Furthermore, $La_2Zr_2O_7$ has favorable thermal conductivity at elevated temperatures, which is ~20% lower than that of YSZ. Failure of $La_2Zr_2O_7$ coating was not observed after the first thermal cycling tests at temperatures >1,200°C and the coating showed thermal stability. Thus, $La_2Zr_2O_7$ is a very promising material for advanced TBCs. Moskal et al. [46] studied a double-ceramic-layered (DCL) coating consisting of monolayer coatings $Nd_2Zr_2O_7$ and 8YSZ. The coatings had ~300 μm thickness and porosities of ~5%. The chemical and phase composition analysis of the DCL layers revealed an external $Nd_2Zr_2O_7$ ceramic layer (~80 μm thick), a transitional zone (~120 μm thick), and an internal 8YSZ layer (100 μm thick). The $Nd_2Zr_2O_7$ pyrochlore phase was the only one-phase component. The surface topography of both TBC systems was typical for plasma sprayed coatings, and compressive stress state had a value in the range of ~5–10 MPa. Measurements of the thermal parameters, i.e., thermal diffusivity indicated better thermal insulation for both new types of layers as compared to the standard 8YSZ layers [46].

Yb_2O_3 (10 mol%) and Gd_2O_3 (20 mol%) doped $SrZrO_3$ was investigated by Ma et al. [47] as a material for TBC applications. Measurement of thermal expansion coefficients (TECs) of sintered bulk $Sr(Zr_{0.9}Yb_{0.1})O_{2.95}$ and $Sr(Zr_{0.8}Gd_{0.2})O_{2.9}$ displayed a positive influence on phase transformations of $SrZrO_3$ by doping Yb_2O_3 or Gd_2O_3. It was observed that both dopants can reduce the thermal conductivity of $SrZrO_3$. Dense $Sr(Zr_{0.9}Yb_{0.1})O_{2.95}$ and $Sr(Zr_{0.8}Gd_{0.2})O_{2.9}$ had lower hardness, Young's modulus, and comparable fracture toughness as compared to YSZ. At operating temperatures <1,300°C, the cycling lifetimes of plasma sprayed $Sr(Zr_{0.9}Yb_{0.1})O_{2.95}$/YSZ and $Sr(Zr_{0.8}Gd_{0.2})O_{2.9}$/YSZ double DLC were comparable to that of YSZ coating. However, at operating temperatures >1,300°C, the cycling lifetime of $Sr(Zr_{0.9}Yb_{0.1})O_{2.95}$/YSZ DLC was about 25% longer than YSZ coating, while that was shorter for $Sr(Zr_{0.8}Gd_{0.2})O_{2.9}$/YSZ DLC compared to YSZ coating [47]. The rare earth zirconates ($M_2Zr_2O_7$, M = La → Gd) have a low intrinsic thermal conductivity and high temperature phase stability, which make them

http://dx.doi.org/10.5772/61346

attractive candidates for TBC applications. Electron-beam evaporation, directed-vapor deposition (EB-DVD) technique was used by Zhao et al. [48] to investigate the synthesis of $Sm_2Zr_2O_7$ (SZO) coatings and to explore the relationships between the deposition conditions and the coating composition, pore morphology, structure, texture, and thermal conductivity. The coatings exhibited significant fluctuations in composition because of the vapor pressure differences of the constituent oxides. It was noticed that the coatings had a metastable fluorite structure due to kinetic limitations that hindered the formation of the equilibrium pyrochlore structure. The morphology of growth of EB-DVD SZO was identical to those of EB-DVD 7YSZ and EB-PVD $Gd_2Zr_2O_7$. The conductivity values of the as-deposited SZO coatings were nearly one-half of their DVD 7YSZ counterparts. This may be ascribed to their lower intrinsic conductivity [48].

Alumina-based ceramic coating with a composition of La_2O_3, Al_2O_3 and MgO ($MMeAl_{11}O_{19}$, M-La, Nd; Me-alkaline earth elements, magnetoplumbite structure) has been developed as TBC by the researchers [49, 50]. Lanthanum hexaaluminate (LHA) coating has long-term structural and thermo-chemical stability of up to 1673 K and significantly lower sintering rate than zirconia-based TBCs. The low thermal conductivity of LHA is ascribed to the random arrangement of LHA platelets leading to micro-porous coating. The insulating properties of the material are related to its crystallographic feature. To meet the demand of advanced turbine engines, $LaTi_2Al_9O_{19}$ (LTA) was proposed and investigated as a novel TBC material for application at 1,300°C by Xie et al. [51]. LTA showed excellent phase stability up to 1,600°C. The thermal conductivities for LTA coating were in a range of 1.0–1.3 W m^{-1} K^{-1} (300–1,500°C). The values of thermal expansion coefficients increased from 8.0 to 11.2 × 10^{-6} K^{-1} (200–1,400°C), which were comparable to those of YSZ. Both the LTA and YSZ coatings had a microhardness value of about 7 GPa, whereas the fracture toughness value was relatively lower than that of YSZ. However, the double-ceramic LTA/YSZ layer design balanced the lower fracture toughness. The LTA/YSZ TBC showed thermal cycling life of ~700 h at 1,300°C [51]. Lathanum phosphate ($LaPO_4$) is considered as a potential TBC material on Ni-based superalloys because of its high temperature stability, high thermal expansion, and low thermal conductivity [52]. Further, lanthanum phosphate is expected to have good corrosion resistance in environments containing sulfur and vanadium salts. However, plasma spraying can not be easily used to make this type of coating. Detailed research is needed to establish the suitability of $LaPO_4$ as TBC. Rare earth oxide coatings (La_2O_3, CeO_2, Pr_2O_3, and Nb_2O_5 as main phases) can be used as TBCs as they have lower thermal diffusivity and higher thermal expansion coefficient than ZrO_2 [53]. Most of the rare earth oxides are polymorphic at elevated temperatures [54] and their phase instability affects the thermal shock resistance of these coatings to a certain extent. When zircon is used as a TBC material, it dissociates during plasma spraying and consequently coatings are composed of a mixture of crystalline ZrO_2 and amorphous SiO_2. For diesel engines, the decomposed SiO_2 in the coating may cause problems due to the evaporation of SiO and $Si(OH)_2$ [55]. The thermal barrier effect is supposed to be due to the ZrO_2 phase in the coating [56]. However, few other silicates such as garnet almandine [$Fe_3Al_2(SiO_4)_3$], garnet pyrope [$Mg_3Al_2(SiO_4)_3$], garnet andradite-grossular [$Ca_3Al_2(SiO_4)_3$], and basalt (glass) have potential as TBC materials [57]. The composite oxide coating consisting of $2CaO.SiO_2$-10 to 30 wt% $CaO.ZrO_2$ shows excellent resistance to thermal shock and hot corrosion [58].

Researchers have conceived garnets [$Y_3Al_xFe_{5-x}O_{12}$ (x=0, 0.7, 1.4, and 5)] as TBC materials [59]. YAG ($Y_3Al_5O_{12}$) has superior high-temperature mechanical properties, low thermal conductivity, excellent phase/thermal stability up to the melting point and significantly lower oxygen diffusivity than those of zirconia. However, the major drawback of this material is its low melting point and relatively low thermal expansion coefficient [59]. Guo et al. [60] produced $BaLa_2Ti_3O_{10}$ (BLT) by solid-state reaction of $BaCO_3$, TiO_2, and La_2O_3 for 48 h at 1,500°C. BLT showed phase stability between room temperature and 1,400°C. BLT showed a linearly increasing thermal expansion coefficient with increasing temperature up to 1,200°C and the coefficients of thermal expansion (CTEs) were in the range of 1×10^{-5}–12.5×10^{-6} K^{-1}, comparable to those of 7YSZ. BLT coatings with stoichiometric composition were developed by APS technique. The coating contained segmentation cracks and had a porosity of ~13%. The microhardness for the BLT coating was in the range of 3.9–4.5 GPa. The thermal conductivity at 1,200°C was about 0.7 W/mK and thereby, revealing it as a promising material in improving the thermal insulation property of TBC. Thermal cycling results showed that the BLT TBC had a lifetime of more than 1,100 cycles of about 200 h at 1,100°C. The failure of the coating occurred by cracking at the TGO layer due to severe bond coat oxidation. Based on the experimental results BLT can be considered as a promising material for TBC applications [60]. Xu et al. [61] deposited DCL TBCs consisting of $La_2(Zr_{0.7}Ce_{0.3})_2O_7$ (LZ7C3) and YSZ by EB-PVD method. They showed that the DCL coating had a much longer lifetime than the single layer LZ7C3 coating and much longer than that of the single layer YSZ coating. Similar thermal expansion behaviors of YSZ interlayer with LZ7C3 coating and TGO layer, high sintering-resistance of LZ7C3 coating and unique columnar growth within DCL coating led to the extension of thermal cycling life of DCL coating. The failure of DCL coating occurred due to the reduction-oxidation of cerium oxide, the crack initiation, propagation and extension, the abnormal oxidation of bond coat, the degradation of *t*′-phase in YSZ coating, and the outward diffusion of Cr alloying element into LZ7C3 coating [61]. Dy_2O_3–Y_2O_3 co-doped ZrO_2 exhibits lower thermal conductivity and higher coefficient of thermal expansion. Thus, it is a promising ceramic thermal barrier coating material for aero-gas turbines and high temperature applications in metallurgical and chemical industry. Qu et al. [62] prepared Dy_2O_3–Y_2O_3 co-doped ZrO_2 ceramics using solid state reaction methods. $Dy_{0.06}Y_{0.072}Zr_{0.868}O_{1.934}$ exhibited a lower thermal conductivity and higher coefficient of thermal expansion as compared with standard 8 wt% Y_2O_3-stabilized ZrO_2 used in conventional TBCs. The compatibility between the TGO (Al_2O_3) and the new compositions is complicated to ensure the durability of TBCs. $Dy_{0.06}Y_{0.072}Zr_{0.868}O_{1.934}$ was found to be compatible with Al_2O_3 whereas $YAlO_3$ and $Dy_3Al_2(AlO_4)_3$ were formed when $Dy_{0.25}Y_{0.25}Zr_{0.5}O_{1.75}$ and Al_2O_3 were mixed and sintered [62].

New alternative TBC materials to YSZ for applications above 1,473 K are being explored by researchers. Zhou et al. [63] prepared $Y_4Al_2O_9$ (YAM) ceramics by solid state reaction at 1,873 K for 12 h. They investigated the phase stability, thermophysical properties, and sintering-resistance behavior of the material. XRD results revealed single monoclinic phase YAM. Even no new phase appeared after long-term annealing. The thermal conductivities of YAM ceramic decreased gradually with the increase of temperature ranges from room temperature to 1,273 K. The minimum value obtained was ~1.81 W m^{-1} K^{-1}, which is lower than that of YSZ. YAM showed moderate thermal expansion coefficient, i.e., 8.91×10^{-6} K^{-1} in the temperature range

of 300–1,473 K. In comparison to YSZ, YAM has lower density and higher sintering-resistance ability, which is very favorable for TBC applications. The results indicated that YAM is a promising ceramic material candidate for application in the TBC system [63]. YSZ is usually used as ceramic top coat for gas turbine blades and vanes. The accelerated phase transformation and the intensified sintering of the YSZ top coat at temperatures between 1,200°C and 1,300°C lead to microstructural changes resulting in higher thermal stress generation and lifetime reduction. Additionally, thermal conductivity (λ) of the top coat increases. Therefore, lanthanum zirconate ($La_2Zr_2O_7$) and gadolinium zirconate ($Gd_2Zr_2O_7$) is being suggested by researchers as a top coat because of their high phase stability up to their melting points and the lower thermal conductivity compared to YSZ. Bobzin et al. [64] deposited single-(SCL) and DCL top coats consisting of 7 wt% yttria-stabilized zirconia (7YSZ), $La_2Zr_2O_7$, or $Gd_2Zr_2O_7$ using the EB-PVD method. They wanted to investigate the temperature-dependent phase behavior and change of thermal conductivity of SCL and DCL top coats, as well as the influence of different top coat materials and architectures on the growth of the TGO. Morphology and coating thickness were determined using SEM. The SCL and DCL systems showed a columnar microstructure with a coating thickness of about 150 μm. The thermal conductivity of SCL and DCL systems was measured between 400°C and 1,300°C by laser flash technique. The XRD of SCL and DCL systems were carried out after isothermal oxidation at 1,300°C. Finally, the TGO phase was identified by XRD and EDS analysis. Correlation between morphology, architecture, coating material, and TGO behavior can give details of oxygen diffusion processes [64].

Investigation of the ZrO_2–$YO_{1.5}$–$TaO_{2.5}$ system reveals several promising aspects for TBC applications. Unique presence of a stable, non-transformable, tetragonal region in this ternary oxide system allows for phase stability to elevated temperatures, e.g.,1,500°C. Yttria- and tantala-containing compositions exhibited significantly high resistance to vanadate corrosion compared to 7YSZ. Further, yttria- and tantala-stabilized zirconia compositions within the non-transformable tetragonal phase field exhibited toughness values comparable or higher than those of 7YSZ and thereby, increasing their stability as TBCs. Pitek and Levi discussed about these promising attributes based on recent experimental works [65]. Liu et al. [66] prepared pyrochlore-type $(La_{0.8}Eu_{0.2})_2Zr_2O_7$ feedstocks by spray drying and used that to produce ceramic thermal barrier coatings. DCL TBCs with a first layer of 8 wt% YSZ and a top layer of $(La_{0.8}Eu_{0.2})_2Zr_2O_7$ were deposited by plasma spraying. Plasma-sprayed $(La_{0.8}Eu_{0.2})_2Zr_2O_7$ coatings were composed of a defect fluorite-type phase and a *t*-ZrO_2 phase. However, after thermal shock tests at 1,250°C for 32 cycles, $(La_{0.8}Eu_{0.2})_2Zr_2O_7$ coatings exhibited a pyrochlore-type structure. The thermal shock failure of DCL $(La_{0.8}Eu_{0.2})_2Zr_2O_7$/YSZ coatings mainly occurred at the interface between the YSZ and $(La_{0.8}Eu_{0.2})_2Zr_2O_7$ layers. However, the TGO layer from the bond coat had no effect on the thermal shock failure [66]. Two kinds of rare earth zirconate $(Sm_{0.5}La_{0.5})_2Zr_2O_7$ and $(Sm_{0.5}La_{0.5})_2(Zr_{0.8}Ce_{0.2})_2O_7$ ceramics were prepared by Hong-song et al. [67] through solid state reaction at 1,600°C for 10 h. They investigated the phase compositions, microstructures, and thermophysical properties of these materials. XRD results confirmed the formation of single phase $(Sm_{0.5}La_{0.5})_2Zr_2O_7$ and $(Sm_{0.5}La_{0.5})_2(Zr_{0.8}Ce_{0.2})_2O_7$ with pyrochlore structure. Dense microstructures of these materials and absence of other phases among the particles were revealed by SEM studies. The TEC of the ceramic increased with the increasing temperature, while the thermal conductivity

decreased. TECs of $(Sm_{0.5}La_{0.5})_2Zr_2O_7$ and $(Sm_{0.5}La_{0.5})_2(Zr_{0.8}Ce_{0.2})_2O_7$ were lower than that of $Sm_2Zr_2O_7$. The CeO_2 addition resulted in the higher TEC of $(Sm_{0.5}La_{0.5})_2(Zr_{0.8}Ce_{0.2})_2O_7$ than those of 8YSZ and $(Sm_{0.5}La_{0.5})_2Zr_2O_7$. Although the TEC of $(Sm_{0.5}La_{0.5})_2Zr_2O_7$ was lower than that of 8YSZ, still it can serve as a TBC. Doping with La_2O_3 or CeO_2 led to phonon scattering resulting in much lower thermal conductivities of $(Sm_{0.5}La_{0.5})_2Zr_2O_7$ and $(Sm_{0.5}La_{0.5})_2(Zr_{0.8}Ce_{0.2})_2O_7$ than that of $Sm_2Zr_2O_7$. In comparison to the thermal conductivity of $(Sm_{0.5}La_{0.5})_2Zr_2O_7$ the thermal conductivity of $(Sm_{0.5}La_{0.5})_2(Zr_{0.8}Ce_{0.2})_2O_7$ was relatively lower. The experimental results showed that $(Sm_{0.5}La_{0.5})_2Zr_2O_7$ and $(Sm_{0.5}La_{0.5})_2(Zr_{0.8}Ce_{0.2})_2O_7$ are novel candidate materials for TBCs in near future [67].

6.2. Composite top coat

A new TBC was developed by Dietrich et al. [68] from a powder mixture of metal and normal glass by using vacuum plasma spraying technique. This type of TBC material had a similar thermal expansion coefficient of a metal substrate. The thermal conductivity of this composite top coat was about two times greater than that of YSZ. Long thermal cycling life of the metal-glass TBC was attributed to high thermal expansion coefficient, good adherence to the bond coat, and absence of open porosity and thereby, preventing the bond coat oxidation from corrosive gases [68]. Majumdar and Jana [69] studied the properties of a TBC prepared from 3 wt% YSZ dispersed in a high temperature resistant alumino-borosilicate glassy matrix. The YSZ-glass composite coating was applied on stainless steel substrate by a simple and cost-effective enameling technique. The thermal gradient of 800 μm thick TBC was found to be 175–180°C after 30 min exposure at 1,000°C. Significant improvement of the gradient to 650–675°C was observed after long exposure of the coated surface at 1,000°C when compressed air cooling was utilized [69]. The spallation of ceramic coating from the bond coat is an important problem for TBC systems. Basically, the spallation is caused by the oxidation and hot corrosion at the interface of the ceramic layer and bond coat. Keyvani et al. [70] investigated the oxidation and hot corrosion behavior of plasma sprayed nanostructured Al_2O_3/YSZ composite TBC coatings on Ni-based (IN-738LC) superalloy substrate and compared it with the conventional YSZ. The coatings were deposited by plasma spray method. High temperature oxidation test at 1,100°C and hot corrosion test at 1,050°C using Na_2SO_4 and V_2O_5 molten salts were conducted on the coatings. The experimental data demonstrated that the nanostructured Al_2O_3/YSZ composite coating had higher oxidation and hot corrosion resistance than those of the conventional YSZ coating. The microstructural analysis indicated that the growth of TGO was much less for this nanostructured Al_2O_3/YSZ composite coating. Further, the composite top coating prevented infiltration of both oxygen and aggressive molten salt [70]. Novel YSZ (6 wt% yttria partially stabilized zirconia)–(Al_2O_3/YAG) (alumina–yttrium aluminum garnet, $Y_3Al_5O_{12}$) DLC coatings were formed by using the composite sol-gel and pressure filtration microwave sintering (PFMS) technologies by Ren et al. [71]. The microstructural observations showed that micro-sized YAG particles were embedded in nano-sized α-Al_2O_3 film. A thin Al_2O_3/YAG layer had good adherence with the substrate and the thick YSZ top layer. Cyclic oxidation tests at 1,000°C indicated that they can resist oxidation of alloy and improve the spallation resistance. The thermal insulation capability tests at 1,000°C and 1,100°C indicated that 250 μm coating had better thermal barrier effect than that of the 150 μm coating at different cooling gas rates. The

http://dx.doi.org/10.5772/61346

decrease in oxidation rate for forming a TGO scale using the sealing effect of α-Al_2O_3 and the reduced thermal stresses by means of nano/micro composite structure led to these beneficial effects. This double-layer coating can be considered as a promising TBC [71].

6.3. Glass-ceramics as TBC materials

$MgO–Al_2O_3–TiO_2$ and $ZnO–Al_2O_3–SiO_2$ based glass-ceramic coatings have been developed as TBCs for gas turbine engine components by Datta and Das [72, 73]. These coatings were formed on nimonic alloy substrates using the vitreous enameling technique. $MgO–Al_2O_3–TiO_2$-based glass coating was applied on nimonic alloy substrate by spraying the glass slurry, drying, and then firing at about 1,160°C for 5–6 min. Further, the glass coating was heat treated for 1 h at 880°C followed by 1 h at 1,020°C to develop crystals such as magnesium aluminum titanate as a major phase along with magnesium silicate and aluminum titanate as minor phases in the glass matrix. The thermal shock resistance of the glass-ceramic coating was found to be more than 10 cycles when repeatedly heated to 750°C and immediately quenched in cold water. No chipping or spalling defect was observed. Slight weight gain was noted during the thermal endurance test at 1,000°C for 100 h. However, the operating temperature of this coating is limited to 750°C. Glass-ceramic coating based on $ZnO–Al_2O_3–SiO_2$ systems can operate at high working temperatures of up to 1,000°C. This type of glass coating was applied on a nimonic alloy through the spraying of a suitable glass slip, drying, and firing at 1,200°C for 5–6 min. The glass coating was subsequently heat treated at 1,000°C for 1 h to develop gahnite, willemite, and cristobalite crystalline phases. Thermal shock at 1,000°C for 10 cycles showed no chipping. During the thermal endurance test at 1,000°C for 100 h, negligible weight gain was observed. Figure 1(a) shows the oxidative weight gain of the bare substrate and $MgO–Al_2O_3–TiO_2$-based glass-ceramic coated substrate during the oxidation test at 1,000°C for 100 h. Typical SEM image of $MgO–Al_2O_3–TiO_2$-based glass-ceramic coating is shown in Figure 2(b).

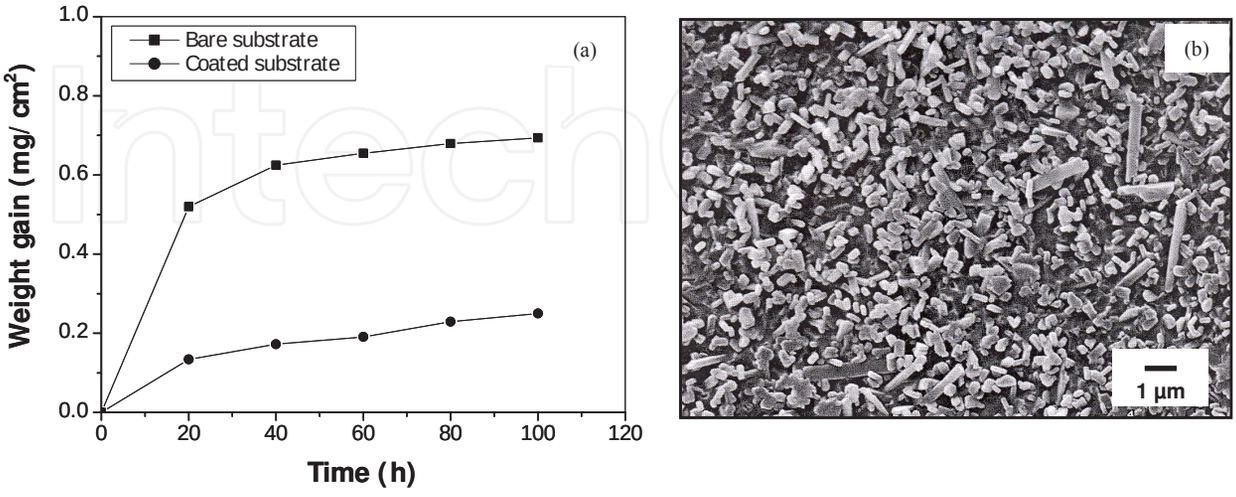

Figure 1. (a) Oxidative weight gain of $MgO–Al_2O_3–TiO_2$-based glass-ceramic coated substrate at 1,000°C for 100 h and (b) typical SEM microstructure of the corresponding coating.

7. Promising bond coat materials for TBC systems

TBCs with ceramic top coat and MCrAlY (M=Ni, Co) bond coat are generally applied on gas turbine engine components to protect them from high temperature exposure [3]. The bond coat provides thermo-elastic relaxation to accommodate the high stresses generated in the TBC system. The chemistry and microstructure of bond coat affects the structure and morphology of the TGO [3]. The oxidation of bond coat needs to be restricted to improve the performance of the TBC system. Glass-ceramics may be used as bond coats because of several reasons. As this bond coat is basically oxide-based, failure of the TBC system from bond coat oxidation may be avoided. Further, high stress may be accommodated by the viscous flow of the glass-ceramics, which may increase the stability of the TBC system during thermal cycling at high operating temperatures. In addition, this TBC system may protect the metallic component from oxidation and creep failure more effectively because of the lower thermal conductivity of glass-ceramics compared to metals. Detailed studies on the TBC system consisting of 8 wt% YSZ (~400 μm) top coat, BaO–MgO–SiO_2-based glass-ceramic bond coat (~100 μm) and nimonic alloy (AE 435) substrate have been carried out by Das [74]. The glass-ceramic bond coat and YSZ top coat were applied on the nimonic alloy substrate by conventional enameling and air plasma spraying techniques, respectively. Figure 2 depicts the typical SEM cross-sectional micrograph of this kind of TBC system, which is composed of BaO–MgO–SiO_2-based glass-ceramic bond coat, 8-YSZ top coat, and nimonic superalloy substrate.

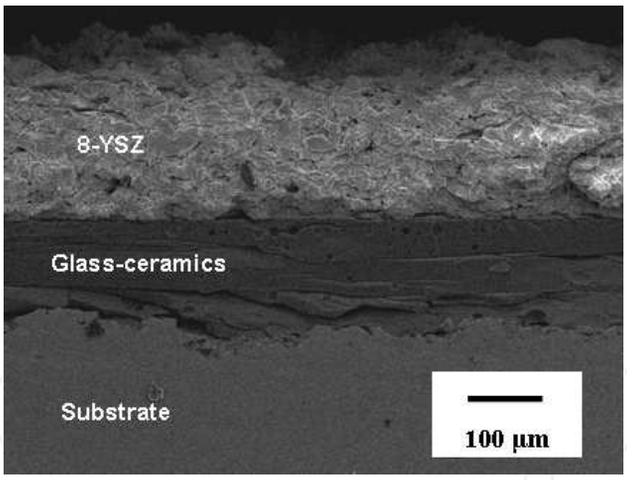

Figure 2. Typical TBC system consisting of glass-ceramic bond coat, 8-YSZ top coat, and nimonic superalloy substrate.

The 90° bend tests on these TBC systems showed that only a small amount of YSZ coating chipped off from the edges, indicating strong adherence of the TBC with the nimonic alloy substrate. The microhardness and Young's modulus values of YSZ coating, glass-ceramic coating, and nimonic alloy substrate of the TBC system were lower on the cross-section than those obtained on the plan-section at a load of 100 mN. The four-point bend test on the TBC system displayed low stiffness (bending elastic modulus−45–52 GPa at room temperature) that leads to low residual stresses in the TBC resulting in high thermo-mechanical stability of the

http://dx.doi.org/10.5772/61346

TBC system [74]. Das et al. [75] studied the oxidation behavior of a TBC system consisting of 8 wt% YSZ top coat, BaO–MgO–SiO_2-based glass-ceramic bond coat, and nimonic alloy (AE 435) substrate wherein static oxidation test was carried out at 1,200°C for 500 h in air. Oxidation resistance of this TBC system was compared with the conventional TBC system under identical heat treatment conditions. Both TBC systems were characterized by SEM, as well as EDS analysis. The TGO layer was not found between the bond coat and the top coat in the case of glass-ceramic bonded TBC system, while the conventional TBC system showed a TGO layer of ~16 μm thickness at the bond coat-top coat interface [75].

Thermal cyclic behavior of glass-ceramic bonded TBC on nimonic alloy substrate was investigated by Das et al. [76]. In that study, a TBC system comprised of 8 wt% YSZ top coat, BaO–MgO–SiO_2-based glass-ceramic bond coat, and nimonic alloy (AE 435) substrate was subjected to thermal shock test from 1,000°C to room temperature for 100 cycles. Specimens held at 1,000°C for 5 min were forced air quenched, as well as water quenched from the same conditions. Microstructural changes were investigated using SEM. The phase analysis was conducted by XRD analysis and EDS analysis. Deterioration was not observed in the top coats after 100 cycles in the case of forced air quenched specimens, whereas the top coats were damaged in the water quenched specimens. After thermal cycling experiments interfacial cracks did not appear at the top coat-bond coat and bond coat-substrate interfaces both in forced air quenched and water quenched specimens. Further, the top coat retained its phase stability [76]. The mechanical properties of a glass-ceramic bonded TBC system have been reported by Ghosh [77].Glass-ceramic bonded TBC showed good thermal gradient property as both the glass-ceramic bond coat and YSZ top coat can act as a thermal barrier to the nimonic alloy substrate and reduce the substrate temperature. The thermal gradient of a TBC-coated substrate was 856°C after 45 min holding of the YSZ coating at 1,200°C. The present TBC prevents the thermal conduction to the nimonic alloy substrate as both the glass-ceramic bond coat and the YSZ top coat have low thermal conductivity. Thermal conductivity measurement showed that the ~100 μm glass-ceramic coated substrate had lower thermal conductivity (~23–27 W/m.K at 1,000°C) than that of the bare nimonic alloy substrate (~28 W/m.K at 1,000°C). Moreover, the thermal conductivity of the glass-ceramic- (~100 μm) and YSZ (~400 μm)-coated nimonic alloy substrate was much lower (17.19 W/m.K at 1,000°C) than that of the bare nimonic alloy substrate (~28 W/m.K at 1,000°C) [74, 78, 79].

Efficient gas turbines can be achieved through the use of engineered components having the capability of operating at higher metal temperatures with longer lifetimes. Gas turbine Inlet temperatures can exceed the melting temperatures of nickel-based superalloys. Advanced air cooling system in association with TBCs can decrease the underlying substrate temperature. NiCoCrAlY overlay coatings are generally used as bond coatings for industrial gas turbines. Extensive research is being carried out to find the suitable bond coat composition. Seraffon et al. [80] reported a new type of bond coat with a wide range of compositions. They focused on the oxidation behavior of the bond coatings at 950°C. A range of Ni–Co–Cr–Al coatings were deposited on sapphire substrates using the physical vapor deposition technique and magnetron sputtering method. Co-sputtering of two targets, such as Ni–10%Cr, Ni–20%Cr, Ni–50%Cr, Ni–20%Co–40%Cr, or Ni–40%Co–20%Cr target, and a pure Al target was used for the

deposition of coatings. The coatings were then oxidized in air for 500 h at 950°C. All samples were characterized by measuring the change in coating thickness using pre- and post-exposure metrology only and also the change in specimen weight. Thick coatings (20–30 μm) were deposited by magnetron sputtering successfully. EDS analysis was used to determine the elemental compositions of the samples. Furthermore, XRD was used to identify the major oxides formed during thermal exposure. The selective growth of protective Cr_2O_3, Al_2O_3 or other less protective mixed oxides was observed. The oxide scale growth rate indicated the suitable coatings that produce more protective oxides and allow future optimization of the bond coating composition for service within the turbine section of industrial gas turbines [80].

In the last decade, it has been observed that Pt-rich γ–γ′ alloys and coatings have good oxidation and corrosion properties. Selezneff et al. [38] used this technique to fabricate doped Pt-rich γ–γ′ bond coatings on AM1® superalloy substrate. These TBC systems were compared with the conventional TBC system composed of a β-(Ni,Pt)Al bond coating. Most of the compositions were superior to the β-(Ni,Pt)Al bond coatings with respect to ceramic top coat adherence and better oxide scale adherence of the γ–γ′-based systems [38]. Iridium modified nickel alluminides are promising bond coats because of their ability to promote α-Al_2O_3 scale growth and to form an oxygen diffusion barrier Ir layer. An innovative Al–Ni–Ir alloy was formulated by Lamastra et al. [81]. A detailed microstructural investigations of both powder and bulk samples were conducted to compare the phase composition, oxidation behavior, and thermal stability of the proposed system with those of the Ir free ones. The AlNiIr system was composed of Al_3Ni_2, $AlNi_3$ and β-NiAl. It was assumed that the presence of Ir promoted the alumina scale growth, which started at ~1000°C. Ni-poor and Al-rich islands were observed in both as cast and oxidized AlNiIr bulk samples. However, Ir had high concentration in Al-rich islands and thereby, suggesting higher affinity of iridium towards Al than Ni. After oxidation at 1,150°C, the α-Al_2O_3 scale growth was observed increasing the TGO thickness with dwelling time. Both Ir ODB and Ir-rich islands at the interface between the alloy and the Al_2O_3 scale were not identified due to the low Ir amount. However, metallic Ir and the compound $Al_{2.75}Ir$ were detected in the powder after thermal treatment at 1,000°C [81].

Developing new bond coat is an effective way to extend the service life of TBCs during high temperature exposure. Yao et al. [82] prepared a novel TBC system composed of an (Al_2O_3–Y_2O_3)/ (Pt or Pt–Au) composite bond coat and a YSZ top coat and Ni-based superalloy by magnetron sputtering and EB-PVD, respectively. Cyclic oxidation tests in air at 1,100°C for 200 h showed that the YSZ top coat and alloy substrate can be bonded together effectively by the (Al_2O_3–Y_2O_3)/(Pt or Pt–Au) composite coating. So, this kind of TBC had excellent oxidation resistance and cracking/buckling resistance, which can be attributed to the sealing effect of such coating. Therefore, the interdiffusion between the bond coat and alloy substrate as well as substrate oxidation can be avoided. The toughening effect of noble metals and composite structure of bond coat resulted in inhibition of the micro-cracks propagation and relaxation of the stress in the bond coat. This ceramic/noble metal composite coating has great prospect for the TBC applications [82]. Wang et al. [83] produced NiAl and NiAlHf/Ru coatings on nickel-based single crystal superalloy in order to investigate the interdiffusion behavior and cyclic oxidation resistance at 1,100°C. Needle-like topologically close-packed phases and secondary

reaction zone (~30 μm thick layer) were formed in the NiAl-coated superalloy after annealing at 1,100°C for 100 h while the precipitates of TCP and SRZ were effectively constrained in the NiAlHf/Ru-coated alloy. The NiAlHf/Ru coating exhibited superior cyclic oxidation resistance as compared to the NiAl coating. They have shown that Ru and Hf have important roles in terms of affecting interdiffusion and cyclic oxidation [83]. Zhang et al [84] developed gradient TBCs consisting of $(Gd_{0.9}Yb_{0.1})_2Zr_2O_7$–yttria-stabilized zirconia (8YSZ) and Hf-doped NiAl bond coat by EB-PVD technique. The effect of the interfacial structure between $(Gd_{0.9}Yb_{0.1})_2Zr_2O_7$ (GYbZ) and 8YSZ layers on the thermal cycling behavior was investigated by comparing the DCL coatings with gradient thermal barrier coatings (GTBCs). The thermal cycling tests showed that the GTBCs had a more extended lifetime than that of the DCL coatings. The failure of GYbZ-8YSZ DCL coating with clear interface between different ceramic layers occurred through delaminating cracking as a result of crack initiation and propagation caused by stress concentration within the ceramic layers. Further, the failure of GTBC occurred due to the thermal expansion mismatch between the Hf-doped NiAl bond coat and the TGO layer [84].

8. Conclusions

In the future, TBCs are required to be more suitably designed for the thermal protection of gas turbine engine components to significantly increase engine operating temperatures, fuel efficiency, and engine reliability. However, coating durability is a vital factor to increase the engine operating temperature. Therefore, the coating behavior and failure modes under high temperature, high thermal gradient cyclic conditions should be properly understood to develop next-generation advanced TBCs.

Acknowledgements

The authors are very grateful to Mr. K. Dasgupta, Director, CSIR-Central Glass and Ceramic Research Institute (CSIR-CGCRI), Kolkata-700 032, India, for his kind permission to publish this book chapter.

Author details

Sumana Ghosh*

Address all correspondence to: sumana@cgcri.res.in

Bio-ceramics and Coating Division, CSIR-Central Glass and Ceramic Research Institute, Kolkata, India

References

[1] Tang F, Ajdelsztajn L, Kim GE, Provenzano V, Schoenung JM. Effects of variations in coating materials and process conditions on the thermal cycle properties of NiCrAlY/YSZ thermal barrier coatings. Materials Science and Engineering A. 2006; 425: 94-106.

[2] Matsumoto M, Takayama H, Yokoe D, Mukai K, Matsubara H, Kagiya Y, Sugita Y. Thermal cycle behavior of plasma sprayed La_2O_3,Y_2O_3 stabilized ZrO_2 coatings. Scripta Materialia. 2006; 54: 2035-2039.

[3] Martena M, Botto D, Fino P, Sabbadini S, Gola MM, Badini C. Modelling of TBC system failure: Stress distribution as a function of TGO thickness and thermal expansion mismatch. Engineering Failure Analysis. 2006; 13: 409-426.

[4] Clarke DR, Oechsner M, Padture NP. Thermal-barrier coatings for more efficient gas-turbine engines. MRS bulletin. 2012; 37: 891-898.

[5] Busso EP, Lin J, Sakurai S, Nakayama M. Mechanistic study of oxidation-induced degradation in a plasma-sprayed thermal barrier coating system. Part I: Model formulation. Acta Materialia. 2001; 49: 1515-1528.

[6] Daroonparvar M, Hussain MS, Yajid MAM. The role of formation of continues thermally grown oxide layer on the nanostructured NiCrAlY bond coat during thermal exposure in air. Applied Surface Science. 2012; 261: 287-297.

[7] Xu R, Fan XL, Zhang WX, Wang TJ. Interfacial fracture mechanism associated with mixed oxides growth in thermal barrier coating system. Surface and Coatings Technology. 2014; 253: 139-147.

[8] Evans HE. Oxidation failure of TBC systems: An assessment of mechanisms. Surface and Coatings Technology. 2011; 206: 1512-1521.

[9] Haynes JA, Ferber MK, Porter WD. Thermal cycling behavior of plasma-sprayed thermal barrier coatings with various MCrAIX bond coats. Journal of Thermal Spray Technology. 2000; 9: 38-48.

[10] Sfar K, Aktaa J, Munz D. Numerical investigation of residual stress fields and crack behavior in TBC systems. Materials Science and Engineering: A. 2002; 333: 351-360.

[11] Yang L, Yang F, Long Y, Zhao Y, Xiong X, Zhao X, Xiao P. Evolution of residual stress in air plasma sprayed yttria stabilised zirconia thermal barrier coatings after isothermal treatment. Surface and Coatings Technology. 2014; 251: 98-105.

[12] Pujol G, Ansart F, Bonino J-P, Malié A, Hamadi S. Step-by-step investigation of degradation mechanisms induced by CMAS attack on YSZ materials for TBC applications. Surface and Coatings Technology. 2013; 237: 71-78.

[13] Thompson JA, Clyne TW. The effect of heat treatment on the stiffness of zirconia top coats in plasma-sprayed TBCs. Acta Materialia. 2001; 49: 1565-1575.

[14] Abubakar AA, Akhtar SS, Arif AFM. Phase field modeling of V_2O_5 hot corrosion kinetics in thermal barrier coatings. Computational Materials Science. 2015; 99: 105-116.

[15] Kulkarni A, Vaidya A, Goland A, Sampath S, Herman H. Processing effects on porosity-property correlations in plasma sprayed yttria-stabilized zirconia coatings. Materials and Engineering A. 2003; 359: 100-111.

[16] Zhang D, Gong S, Xu H, Wu Z. Effect of bond coat surface roughness on the thermal cyclic behavior of thermal barrier coatings. Surface & Coatings Technology. 2006; 201: 649-653.

[17] Movchan BA, Yakovchuk YK. Graded thermal barrier coatings, deposited by EB-PVD. Surface & Coatings Technology 2004;188-189: 85-92.

[18] Wu LT, Wu RT, Zhao X, Xiao P. Microstructure parameters affecting interfacial adhesion of thermal barrier coatings by the EB-PVD method. Materials Science & Engineering: A. 2014; 594: 193-202.

[19] Basu SN, Ye G, Gevelber M, Wroblewski D. Microcrack formation in plasma sprayed thermal barrier coatings. International Journal of Refractory Metals & Hard Materials. 2005; 23: 335-343.

[20] Bengtsson P, Johanneson TJ. Characterization of microstructural defects in plasma sprayed thermal barrier coatings. Journal of Thermal Spray Technology. 1995; 4: 245-251.

[21] Chen WR, Wu X, Dudzinski D, Patnaik PC. Modification of oxide layer in plasma sprayed thermal barrier coatings. Surface & Coatings Technology. 2006; 200: 5863-5868.

[22] Tang F, Schoenung JM. Evolution of Young's modulus of air plasma sprayed yttria-stabilized zirconia in thermally cycled thermal barrier coatings. Scripta Materialia. 2006; 54: 1587-1592.

[23] Basu D, Funke C, Steinbrech RW. Effect of heat treatment on elastic properties of separated thermal barrier coatings. Journal of Materials Research. 1999; 14: 4643-4650.

[24] Limargaa AM, Widjajab TS, Yip TH. Mechanical properties and oxidation resistance of plasma-sprayed multilayered Al_2O_3/ZrO_2 thermal barrier coatings. Surface & Coatings Technology. 2005; 197: 93-102.

[25] Guo HB, Kuroda S, Murakami H. Segmented thermal barrier coatings produced by atmospheric plasma spraying hollow powders. Thin Solid Films. 2006; 506-507: 136-139.

[26] Chen X, Gu L, Zou B, Wang Y, Cao X. New functionally graded thermal barrier coating system based on $LaMgAl_{11}O_{19}$/YSZ prepared by air plasma spraying. Surface & Coatings Technology. 2012; 206: 2265-2274.

[27] Préauchat B, Drawin S. Properties of PECVD-deposited thermal barrier coatings. Surface & Coatings Technology. 2001; 142-44: 835-842.

[28] Vyas JD, Choy K-L. Structural characterisation of thermal barrier coatings deposited using electrostatic spray assisted vapour deposition method. Materials Science and Engineering: A. 2000; 277: 206-212.

[29] Gell M, Xie L, Ma X, Jordan EH, Padture NP. Highly durable thermal barrier coatings made by the solution precursor plasma spray process. Surface and Coating Technology. 2004; 177-178: 97-102.

[30] Jadhav A, Padture NP, Wu F, Jordan EH, Gell M. Thick ceramic thermal barrier coatings with high durability deposited using solution-precursor plasma spray. Materials Science and Engineering: A. 2005; 405: 313-320.

[31] Viazzi C, Bonino JP, Ansart F. Synthesis by sol–gel route and characteri-zation of yttria stabilized zirconia coatings for thermal barrier applications. Surface & Coatings Technology. 2006; 201: 3889-3893.

[32] Sniezewski J, Le MY, Lours P, Pin L, Minvie BV, Monceau D, Oquab D, Fenech J, Ansart F, Bonino J-P. Sol–gel thermal barrier coatings: Optimization of the manufacturing route and durability under cyclic oxidation. Surface & Coatings Technology. 2010; 205:1256-1261.

[33] Pin L, Ansart F, Bonino J-P, Maoult YL, Vidal V, Lours P. Processing,repairing and cyclic oxidation behaviour of sol–gel thermal barrier coatings. Surface & Coatings Technology. 2011; 206:1609-1614.

[34] Pin L, Ansart F, Bonino J-P, Le Maoult Y, Vidal V, Lours P. Reinforcedsol–gel thermal barrier coatings and their cyclic oxidation life. Journal of the European Ceramic Society. 2013; 33: 269-276.

[35] Ren C, He YD, Wang DR. Cyclic oxidation behavior and thermal barrier effect of YSZ–(Al_2O_3/YAG) double-layer TBCs prepared by the composite sol–gel method. Surface & Coatings Technology. 2011; 206: 1461-1468.

[36] Monceau D, Oquab D, Estournes C, Boidot M, Selezneff S, Thebault Y, Cadoret Y. Pt-modified Ni aluminides, MCrAlY-base multilayer coatings and TBC systems fabricated by Spark Plasma Sintering for the protection of Ni-base superalloys. Surface & Coatings Technology. 2009; 204: 771-778.

[37] Boidot M, Selezneff S, Monceau D, Oquab D, Estournès C. Proto-TGO formation in TBC systems fabricated by spark plasma sintering. Surface & Coatings Technology. 2010; 205: 1245-1249.

[38] Selezneff S, Boidot M, Hugot J, Oquab D, Estournès C, Monceau D. Thermal cycling behavior of EBPVD TBC systems deposited on doped Pt-rich γ–γ′ bond coatings made by Spark Plasma Sintering (SPS). Surface & Coatings Technology. 2011; 206: 1558-1565.

[39] Rousseau F, Fourmond C, Prima F, Serif MHV, Lavigne O, Morvan D, Chereau P. Deposition of thick and 50% porous YpSZ layer by spraying nitrate solution in a low pressure plasma reactor. Surface & Coatings Technology. 2011; 206: 1621-1627.

[40] Ramachandran CS, Balasubramanian V, Ananthapadmanabhan PV. Synthesis, spheroidization and spray deposition of lanthanum zirconate using thermal plasma process. Surface & Coatings Technology. 2012; 206: 3017-3035.

[41] Bahadori E, Javadpour S, Shariat MH, Mahzoon Fatemeh. Preparation and properties of ceramic Al_2O_3 coating as TBCs on MCrAly layer applied on Inconel alloy by cathodic plasma electrolytic deposition. Surface & Coatings Technology. 2013; 228: S611-S614.

[42] Kim JH, Kim MC, Park CG. Evaluation of functionally graded thermal barrier coatings fabricated by detonation gun spray technique. Surface & Coatings Technology. 2003; 168: 275-280.

[43] Chwa SO, Akira O. Microstructures of ZrO_2-8wt.%Y_2O_3 coatings prepared by a plasma laser hybrid spraying technique. Surface & Coatings Technology. 2002; 153: 304-312.

[44] Wang W, Li C, Li J, Fan J, Zhou X. Effect of gadolinium doping on phase transformation and microstructure of Gd_2O_3-Y_2O_3-ZrO_2 composite coatings prepared by electrophoretic deposition. Journal of Rare Earths. 2013; 31: 289-295.

[45] Vassen R, Cao X, Tietz F, Basu D, Sto°ver D. Zirconates as new materials for thermal barrier coatings. Journal of the American Ceramic Society. 2000; 83: 2023-2028.

[46] Moskal G, Swad´zba L, Hetma´nczyk M, Witala B, Mendala B, Mendala J, Sosnowy P. Characterization of microstructure and thermal properties of $Gd_2Zr_2O_7$-type thermal barrier coating. Journal of the European Ceramic Society 2012; 32: 2025-2034.

[47] Ma W, Mack D, Malzbender J, Vaßen R, St°over D. Yb_2O_3 and Gd_2O_3 doped strontium zirconate for thermal barrier coatings. Journal of the European Ceramic Society. 2008; 28: 3071-3081.

[48] Zhao H, Levi CG, Wadley HNG. Vapor deposited samarium zirconate thermal barrier coatings. Surface & Coatings Technology. 2009; 203: 3157-3167.

[49] Vassen R, Cao X, Dietrich M, Stoever D. Improvement of new thermal barrier coating systems using layered or graded structure. In: Singh M, Jessen T (Eds.) The 25th Annual International Conference on Advanced Ceramics and Composites: An Advanced Ceramics Odyssey, Cocoa Beach of Florida: American Ceramic Society; 2001. p 435.

[50] Friedrich CJ, Gadow R, Lischka MH. Lanthanum hexaaluminate thermal barrier coatings. In: Singh M, Jessen T (Eds.) The 25th Annual International Conference on Composites, Advanced Ceramics, Materials, and Structures: B, Cocoa Beach of Florida: American Ceramic Society; 2001. p 372-375.

[51] Xie X, Guoa H, Gonga S, Xu H. Lanthanum–titanium–aluminum oxide: A novel thermal barrier coating material for applications at 1300°C. Journal of the European Ceramic Society. 2011; 31: 1677-1683.

[52] Sudre O, Cheung J, Marshall D, Morgan P, Levi CG. Thermal insulation coatings of $LaPO_4$. In: Singh M, Jessen T (Eds.) The 25th Annual International Conference on Composites, Advanced Ceramics, Materials,and Structures: B, Cocoa Beach of Florida: American Ceramic Society; 2001. p 367.

[53] Ding C, Xi Y, Zhang Y, Qu J, Qiao, H. Thermophysical properties of plasma sprayed rare earth oxide coatings. In: Sandmeier S, Eschnauer H, Huber P, Nicoll AR. (Eds.) The 2nd Plasma-technik-symposium (Lucerne Switzerland, June 1991), Switzerland: Plasma-Technik AG, Wohlen; 1991. p 27-32.

[54] Warshaw I, Roy R. Polymorphism of the rare earth sesquioxides. The Journal of Physical Chemistry. 1965; 65: 2048-2051.

[55] Kvernes I, Lugscheider E, Ladru F. Lifetime and degradation processes of TBCs for diesel engines. In: Lecomte-Beckers J, Schuber F, Ennis PJ. (Eds.) Proceedings of the 6th Lie´ge Conference on Materials for Advanced Power Engineering (Universite de Lie´ge, Belgium), Forschungszentrum Ju° lich GmbH, Ju° lich; 1998. p 997-1001.

[56] Ramaswamy P, Seetharamu S, Varma KB, Rao KJ. Thermal barrier coating application of zircon sand. Journal of Thermal Spray Technology. 1999; 8: 447-453.

[57] Chra´ ska P, Neufuss K, Kolman B, Dubsky J. Plasma spraying of silicates. In: Berndt CC. (Ed.) Proceedings of the 1st United Thermal Spray Conference: Thermal Spray—A United Forum for Scientific and Technological Advances, Indiana USA: ASM International, Materials Park; 1997. p 477-481.

[58] Morgan PED, Marshall DB. Ceramic composites of monayite and alumina. Journal of the American Ceramic Society 1995; 78: 1553-1563.

[59] Nitin PP, Klemens PG. Low thermal conductivity in garnets. Journal of the American Ceramic Society. 1977; 80: 1018-1020.

[60] Guo H, Zhang H, Ma G, Gong S. Thermo-physical and thermal cycling properties of plasma-sprayed $BaLa_2Ti_3O_{10}$ coating as potential thermal barrier materials. Surface & Coatings Technology. 2009; 204: 691-696.

[61] Xu Z, He, S, He L, Mu R, Huang G, Cao X. Novel thermal barrier coatings based on $La_2(Zr_{0.7}Ce_{0.3})_2O_7$/8YSZ double-ceramic-layer systems deposited by electron beam physical vapor deposition. Journal of Alloys and Compounds. 2011; 509: 4273-4283.

[62] Qu L, Choy K-L, Thermophysical and thermochemical properties of new thermal barrier materials based on Dy_2O_3–Y_2O_3 co-doped zirconia. Ceramics International. 2014; 40: 11593-11599.

[63] Zhou X, Xu Z, Fan X, Zhao S, Cao X, He L. $Y_4Al_2O_9$ ceramics as a novel thermal barrier coating material for high-temperature applications. Materials Letters. 2014; 134:146-148.

[64] Bobzin K, Bagcivan N, Brögelmann T, Yildirim B. Influence of temperature on phase stability and thermal conductivity of single- and double-ceramic-layer EB–PVD TBC top coats consisting of 7YSZ, $Gd_2Zr_2O_7$and $La_2Zr_2O_7$. Surface and Coatings Technology. 2013; 237: 56-64.

[65] Pitek FM, Levi CG. Opportunities for TBCs in the ZrO_2–$YO_{1.5}$–$TaO_{2.5}$ system. Surface and Coatings Technology. 2007; 201: 6044-6050.

[66] Liu Z-G, Zhang W-H, Ouyang J-H, Zhou Y. Novel double-ceramic-layer $(La_{0.8}Eu_{0.2})_2Zr_2O_7$/YSZ thermal barrier coatings deposited by plasma spraying. Ceramics International. 2014; 40: 11277-11282.

[67] Hong-song Z, Qiang X, Fu-chi W, Ling L, Yuan W, Xiaoge C. Preparation and thermophysical properties of $(Sm_{0.5}La_{0.5})_2Zr_2O_7$ and $(Sm_{0.5}La_{0.5})_2$ $(Zr_{0.8}Ce_{0.2})_2O_7$ ceramics for thermal barrier coatings. Journal of Alloys and Compounds. 2009; 475: 624-628.

[68] Dietrich M, Verlotski V, Vassen R, Stoever D. Metal-glass based composites for novel TBC-systems. Materials Science and Engineering Technology. 2001; 32: 669-672.

[69] Majumdar A, Jana S. Yttria doped zirconia in glassy matrix useful for thermal barrier Coating. Materials Letters. 2000; 44:197-202.

[70] Keyvani A. Microstructural stability oxidation and hot corrosion resistance of nanostructured Al_2O_3/YSZ composite compared to conventional YSZ TBC coatings. Journal of Alloys and Compounds. 2015; 623: 229-237.

[71] Ren C, He YD, Wang DR. Cyclic oxidation behavior and thermal barrier effect of YSZ–(Al_2O_3/YAG) double-layer TBCs prepared by the composite sol–gel method. Surface and Coatings Technology. 2011; 206: 1461-1468.

[72] Datta S, Das S. A new high temperature resistant glass-ceramic coating for gas turbine engine components. Bulletin of Materials Science 2005; 28: 689-696.

[73] Datta S, Das S. A new high temperature resistant glass-ceramic coating developed in CGCRI, Kolkata. Transactions of the Indian Ceramic Society. 2005; 64: 25-32.

[74] Das S. Study of structure and property relationship in thermal barrier coating system. Ph.D. thesis, Jadavpur University, Kolkata, 2010.

[75] Das S, Datta S, Basu D, Das GC. Glass-ceramics as oxidation resistant bond coat in thermal barrier coating system. Ceramics International. 2009; 35: 1403-1406.

[76] Das S, Datta S, Basu D, Das GC. Thermal cyclic behavior of glass-ceramic bonded thermal barrier coating on nimonic alloy substrate. Ceramics International. 2009; 35: 2123-2129.

[77] Ghosh S. Microstructure and mechanical properties of a glass-ceramic bond coated TBC system. Procedia Materials Science. 2014; 6: 425-429.

[78] Ghosh S. Thermal behavior of glass-ceramic bond coat in a TBC system. Vacuum. 2014; 101: 367-370.

[79] Ghosh S. Thermal properties of glass-ceramic bonded thermal barrier coating system. Transactions of Nonferrous Metals Society of China. 2015; 25: 457-464.

[80] Seraffon M, Simms NJ, Sumner J, Nicholls JR. The development of new bond coat compositions for thermal barrier coating systems operating under industrial gas turbine conditions. Surface and Coatings Technology. 2011; 206: 1529-1537.

[81] Lamastra FR, Cacciotti I, Bellucci A, Nanni F. Innovative Al–Ni–Ir alloy for bond coats: Microstructure, phase analysis and oxidation behaviour. Intermetallics. 2012; 22: 241-250.

[82] Yao J, He Y, Wang D, Peng H, Guo H, Gong S. Thermal barrier coatings with (Al_2O_3–Y_2O_3)/(Pt or Pt–Au) composite bond coat and 8YSZ top coat on Ni-based superalloy. Applied Surface Science. 2013; 286: 298-305.

[83] Wang D, Peng H, Gong S, Guo H. NiAlHf/Ru: Promising bond coat materials in thermal barrier coatings for advanced single crystal superalloys. Corrosion Science. 2014; 78: 304-312.

[84] Zhang H, Guo L, Ma Y, Peng H, Guo H, Gong S. Thermal cycling behavior of $(Gd_{0.9}Yb_{0.1})_2Zr_2O_7$/8YSZ gradient thermal barrier coatings deposited on Hf-doped NiAl bond coat by EB-PVD. Surface and Coatings Technology. 2014; 258: 950-955.